Synthetic Amphiphilic Peptide Models for Protein Ion Channels

J. D. LEAR, Z. R. WASSERMAN, W. F. DEGRADO

Ion channel proteins are important for the conduction of ions across biological membranes. Recent analyses of their sequences have suggested that they are composed of bundles of α-helices that associate to form ion-conducting channels. To gain insight into the mechanisms by which α-helices can aggregate and conduct ions, three model peptides containing only leucine and serine residues were synthesized and characterized. A 21-residue peptide, H_2N-(Leu-Ser-Ser-Leu-Leu-Ser-Leu)$_3$-$CONH_2$, which was designed to be a membrane-spanning amphiphilic α-helix, formed well-defined ion channels with ion permeability and lifetime characteristics resembling the acetylcholine receptor. In contrast, a 14-residue version of this peptide, which was too short to span the phospholipid bilayer as an α-helix, failed to form discrete, stable channels. A third peptide, H_2N-(Leu-Ser-Leu-Leu-Leu-Ser-Leu)$_3$-$CONH_2$, in which one serine per heptad repeat was replaced by leucine, produced proton-selective channels. Computer graphics and energy minimization were used to create molecular models that were consistent with the observed properties of the channels.

ION CHANNELS ARE PROTEINS THAT PARTICIPATE IN THE generation and transmission of electrical activity in the nervous system and also in the hormonal regulation of cellular processes (*1*). A number of physiologically important channel proteins have been cloned and sequenced (*2–7*). The molecular architectures of these proteins, as deduced from hydrophobicity profiles of the amino acid sequences, have many similarities. All of the channel proteins are composed of four or five homologous domains or subunits, each of which appears to contain numerous membrane-spanning α-helices. One or more of these proposed α-helices on each subunit contains polar residues in addition to apolar residues, and the polar residues line up along one face of the helix forming a hydrophilic patch. In structural models for the assembled, functional proteins (Fig. 1A), the polar faces of α-helical segments from neighboring subunits aggregate to form an ion-conducting pore (*8*). The degree of polarity of the side chains involved in pore formation differs from model to model. In some models, highly charged, amphiphilic α-helical segments are believed to line the pore, whereas other, more recent models invoke amphiphilic α-helices with less polar faces, composed primarily of Ser, Thr, and Cys residues (*9*).

Studies with several natural peptides such as alamethicin (*10*) and melittin (*11*) suggest that small, amphiphilic α-helices may aggregate to form ion channels. However, only 2 of the 20 residues in the sequence of alamethicin contain side chains bearing polar groups (Gln^7 and Glu^{18}), and this peptide also contains eight α-aminoisobutyric acid residues. This amino acid has conformational and packing properties that differ markedly from the commonly occurring, chiral amino acids found in proteins (*12*). Melittin, a 26-residue peptide from bee venom, is amphiphilic and has been reported to form multistate ion channels, but these channels appear to vary over two orders of magnitude in their conductances (*13*). Furthermore, the complex sequences of natural peptides make it difficult to determine which side chains or structural features are important for function. Some "designed" synthetic peptides have also been reported to form ion channels (*14*), but channel characterization at the level of detail needed for comparison to natural channel proteins has been lacking. Thus we designed some model peptides and characterized their ion conduction properties, and found that these peptides embody many of the features thought to be required for conduction of ions through the presumed aggregates of α-helical segments occurring in natural ion channel proteins.

Design and synthesis of model ion channels. Several features were included in our design of ion channel peptides. A peptide should be approximately 20 residues in length to provide a helix that can span the hydrocarbon portion of the lipid bilayer. The helix should be amphiphilic to provide the desired transmembrane aggregation of polar faces, but also should have a high degree of hydrophobicity to allow partitioning into the membrane in a vertical orientation (*15*). Finally, the peptide sequence should be simple and repetitive for structural interpretation of channel properties. Leucine was chosen for the apolar face of the helix because of its high hydrophobicity (*16*) and helix-forming propensity (*17*). Serine was chosen for the polar face of the helix because it is polar but uncharged, satisfying the design requirement for a high overall hydrophobicity. A sequence repeat of seven residues was chosen to provide registry of the polar and apolar faces in linked heptamers. Two different sequence repeats, LSSLLSL and LSLLLSL (L, leucine; S, serine), were chosen to explore the effect of the ratio of polar to apolar residues on channel properties (Fig. 1, B and C). We synthesized the 21-residue peptides of each heptameric repeat, which provided peptides long enough to span lipid bilayers as helices, and we made a dimer of the LSSLLSL sequence to test the proposed length requirement for ion channel function.

The peptides were synthesized by coupling protected segments on a solid support. The protected heptamers were prepared with a *p*-nitrobenzophenone oxime resin support (*18*). Purified heptamers were then attached to a *p*-methylbenzhydrylamine resin and dimerized or trimerized with the use of diisopropylcarbodiimide-hydroxybenzotriazole as a coupling agent. The peptides were cleaved from the support and deprotected with anhydrous HF, and purified by reversed-phase high-performance liquid chromatography (HPLC). High peptide purity was essential for obtaining reproducible chan-

The authors are at the Central Research and Development Department, E. I. du Pont de Nemours and Company, Wilmington, DE 19898.

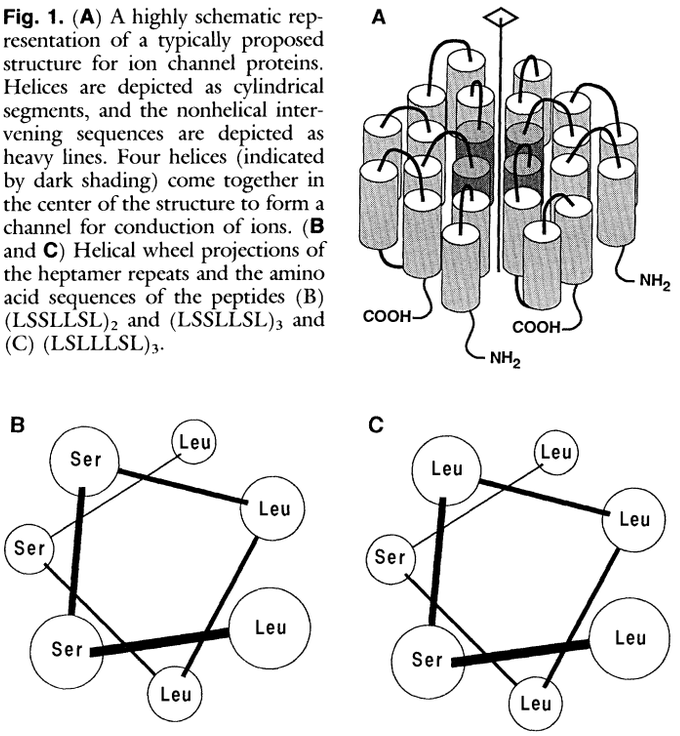

Fig. 1. (**A**) A highly schematic representation of a typically proposed structure for ion channel proteins. Helices are depicted as cylindrical segments, and the nonhelical intervening sequences are depicted as heavy lines. Four helices (indicated by dark shading) come together in the center of the structure to form a channel for conduction of ions. (**B** and **C**) Helical wheel projections of the heptamer repeats and the amino acid sequences of the peptides (B) $(LSSLLSL)_2$ and $(LSSLLSL)_3$ and (C) $(LSLLLSL)_3$.

nel recordings. Peptides that appeared homogeneous by gradient HPLC were found to contain impurities that could be resolved by isocratic reversed-phase HPLC. Only peptides that were homogeneous by this criterion as well as by fast atom bombardment mass spectrometry gave channel records suitable for analysis.

The circular dichroism spectra of the peptides at 25 μM in methanol were typical of α-helical peptides, with a double minimum at 208 and 222 nm (± 2 nm) and a maximum at 190 nm (*19*). Mean residue molar ellipticities at 222 nm were −27,000 degree cm^2/dmole for both 21-residue peptides and −21,000 degree cm^2/dmole for the 14-residue peptide.

$(LSSLLSL)_3$ forms ion channels. The Mueller-Montal planar bilayer method (*20*) was used to determine whether the model peptides formed ion channels in diphytanoyl phosphatidylcholine bilayer membranes. This technique involves the formation of a phospholipid bilayer across a pinhole orifice in a thin film of Teflon that separates two aqueous electrolyte solutions. Application of a voltage across a typical bilayer (Fig. 2A; 100-mV transmembrane voltage) gives rise to little current, indicating that the bilayer greatly impedes the diffusion of ions between aqueous compartments. Incorporation of the 14-residue peptide, $(LSSLLSL)_2$, into the bilayer (*20*) gave rise to erratic increases in current across the membrane (Fig. 2B); similar traces have been observed for a variety of membrane-disruptive agents such as detergents and melittin (*21*). Evidently, this peptide is capable of interacting with phospholipid bilayers, but is too short to form stable, discrete transmembrane ion channels. In contrast, the longer peptide, $(LSSLLSL)_3$, produced the square-wave current pulses characteristic of transmembrane channels (Fig. 2C) switching between conductive and nonconductive states.

The detailed characteristics of the ion channels formed by $(LSSLLSL)_3$ were further examined by computer analysis of a large number of single channel openings (*22*). A histogram illustrating the channel conductance frequency distribution in 0.5*M* KCl showed a major peak at 70 pS (4.3×10^7 ions per second, Fig. 3A), indicating that the channels formed by these peptides had one

Table 1. Comparison of channel characteristics. The conductance values for the muscle end-plate acetylcholine receptor and giant squid nerve sodium channel were measured under physiological conditions (*34*). The $(LSSLLSL)_3$ channel conductance was calculated for 0.15*M* KCl concentration and 100-mV transmembrane potentials by interpolation of data at 0.1 and 0.5*M* KCl and voltages between 50 and 150 mV. The state reported corresponds to the dominant state observed (*23*). The open-state lifetimes correspond to single exponential decay parameters calculated for the acetylcholine receptor of rat embryonic muscle cells (*35*), the sodium channel of neuroblastoma cells (*36*), and $(LSSLLSL)_3$ channels in 0.5*M* KCl.

Characteristic	Channel		
	$(LSSLLSL)_3$ peptide	Acetylcholine receptor	Sodium channel
Conductance (pS)	21	28	*7*
Open-state lifetime (ms)	4	23	0.5
Permeability relative to Na^+*			
H^+	5		
Li^+	0.9	0.86	1.0
Na^+	1.0	1.0	1.0
K^+	1.2	1.11	0.08
Cs^+	1.2	1.42	0.016
Guanidinium$^+$	1.3	1.59	
Tris$^+$	0.3	0.18	
Glucosammonium$^+$	<0.01	0.03	

*Natural channel ion selectivity ratios, determined by reversal potential measurements, are for the end-plate acetylcholine receptor (*37*) and squid axon sodium channel [from summary in (*34*)]. Peptide channel selectivities could not be determined from reversal potentials because the frequency of channel formation was so strongly voltage dependent and also because the single channel conductance was itself voltage dependent. Instead, relative selectivities (estimated error, ±15 percent) were calculated as ratios of single channel conductances at the peak value of histograms. Values for Li^+ and Cs^+ were determined under biionic conditions with 0.5*M* NaCl constant on the negative potential side of the bilayer. Values for tris$^+$ and glucosamine$^+$ were determined by partially replacing the 0.5*M* KCl on the positive side of the bilayer with a 0.5*M* solution of tris·HCl or glucosamine·HCl and observing the resulting change in the single channel conductance. Chloride conductance was less than one-tenth of the total, as judged by data in which the single channel conductance changed from 85 to 45 pS when the KCl concentration was reduced from 0.5 to 0.28*M* on the side of the membrane that was held at 100-mV positive potential.

predominant conductance state, although lower conductance channels were observed to varying degrees in different records (*23*). Measured frequency distributions of the time that channels remained open (Fig. 3B) and of the time between channel openings (Fig. 3C) were well described by single exponentials, suggesting that stochastic, first-order processes were involved in channel opening and closing (*24*). The average open lifetime of the $(LSSLLSL)_3$ channels, as measured by the decay constant for the exponential distribution, was between 3 and 8 ms for most experiments, and no systematic changes in lifetime were evident over a wide range of transmembrane voltages (25 to 175 mV) with several different salts (HCl, LiCl, NaCl, KCl, and CsCl) in concentrations ranging from 0.1 to 0.5*M*. In contrast, the time between channel openings depended on the transmembrane voltage and on the peptide concentration (*25*). At a given peptide concentration, the frequency of channel openings increased when the voltage was increased, indicating that a significant reorientation of electrical dipole accompanies channel formation (*26*). Also, channels occurred far more frequently when the voltage was held negative on the side of the bilayer to which the peptide had been added, an indication of an asymmetric orientation of the peptides in the bilayer.

The ion selectivity of the channels was investigated by measuring conductance distributions with different chloride salts as electrolytes. The channel conductances observed for HCl, LiCl, NaCl, KCl, and CsCl were approximately proportional to the conductances of the corresponding cations in aqueous solution, suggesting that the channels were cation selective. The cation selectivity was confirmed in experiments in which there were (i) different concentrations of

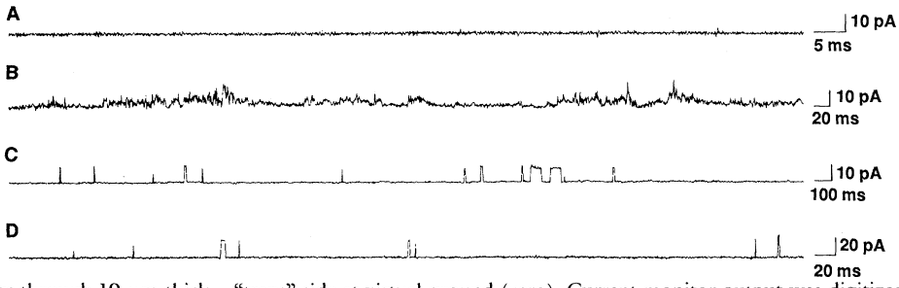

Fig. 2. Single channel data record examples for (**A**) diphytanoyl phosphatidylcholine bilayers and for such bilayers incorporating the synthetic peptides (**B**) $(LSSLLSL)_2$, (**C**) $(LSSLLSL)_3$, and (**D**) $(LSLLLSL)_3$. Peptides were incorporated (*20*) into planar bilayers of diphytanoyl phosphatidylcholine (Avanti Polar Lipids) separating 2 ml of 0.5*M* NaCl or 0.5*M* HCl for $(LSLLLSL)_3$. Bilayers of approximately 100-pF capacitance and >1000-gigohm resistance were formed by monolayer apposition across approximately 100-μm-diameter holes that were pretreated with a squalene-pentane solution and made by electrical discharge through 19-μm-thick polytetrafluoroethylene film (Dielectrix Corp.). Bilayer conductance was monitored under voltage clamp conditions with the 100 mV/pA setting on a List EPC-7 amplifier (Medical Systems Inc.) with an eight-pole, low-pass Bessel filter (Frequency Devices Inc.) setting of 1.6 kHz. Wire electrodes of Ag/AgCl were used without salt bridges. Voltages are defined with the "trans" side at virtual ground (zero). Current monitor output was digitized at 16 kHz (Data Translation DT-2821-F-8DI A/D Board) and processed with C language programs (*22*). The displays are processed only to the extent of connecting successively displayed data points with lines. $(LSSLLSL)_2$ records, which lack defined single channels, were chosen to represent conductance activity in the single channel range.

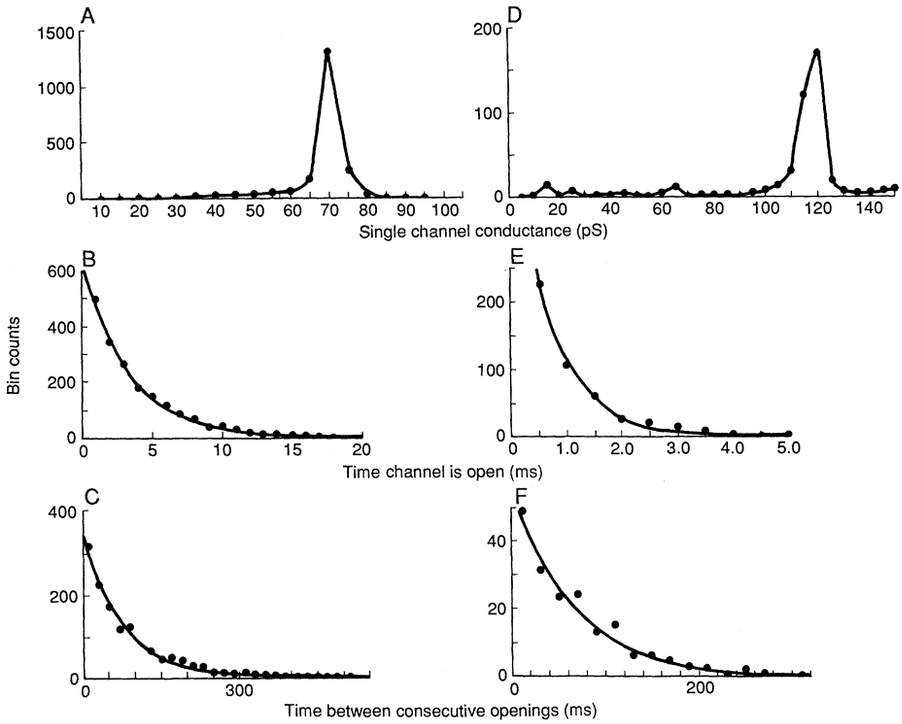

Fig. 3. Histograms of single channel conductances (**A** and **D**), open state (**B** and **E**), and closed state (**C** and **F**) lifetimes for $(LSSLLSL)_3$ and $(LSLLLSL)_3$, respectively. Data for $(LSSLLSL)_3$ were recorded with 0.5*M* KCl, cis-incorporated peptides, and a holding potential of −100 mV (*22*); data for $(LSLLLSL)_3$ were recorded with 0.5*M* HCl, cis-incorporated peptides, and a holding potential of −120 mV. Conductance was calculated as current (in picoamperes above baseline) divided by the transmembrane voltage. Data files of conductance, open times, and closed times were sorted by counting events within 5-pS conductance and 1-ms duration intervals; histogram points are defined as counts between lower and upper limits of the characteristic with the lower limit used as the numerical value of the axis. Solid curves are least-squares fitted single exponential decay curves for the open time durations.

the same chloride salt or (ii) identical concentrations of different cation chloride salts on the two sides of the bilayer (in both cases, under transmembrane potentials greater than twice the calculated maximum reversal potential, the flux of ions due to concentration gradients alone would make a very small contribution). For example, reducing the KCl concentration on only the positive side of the bilayer resulted in a proportional decrease in the conductance (Table 1), indicating that cation flow from the positive to the negative side of the bilayer was responsible for the observed current. Furthermore, the observed conductances of the channels depended on the nature of the cations on the positive, but not the negative, side of the membrane (Table 1). In separate experiments with the same concentration of KCl on both sides of the bilayer, channel conductance was linearly dependent on the potassium ion concentration for 0.1 and 0.5*M* KCl solutions. Taken together with the high magnitude of the rates of conduction, this would indicate that the potassium ions pass through the channels without encountering any significant energy barriers or falling into any deep energy wells.

The effective diameter of the channel conducting region was estimated with hydrochloride salt solutions of guanidine, tris-hydroxymethylaminomethane (tris), and glucosamine. Single channels measured with 0.5*M* guanidinium chloride had conductances very close to those measured for the alkali metal salts, indicating a channel larger than the approximately 5 Å diameter of the guanidinium ion. Substitution of 0.5*M* tris-HCl (approximately 7 Å diameter) reduced channel conductance by a factor of about 4, which would suggest a channel diameter of about 8 Å based on theoretical treatments of ion flux in water-filled pores (*27*). This result is consistent with the finding that the glucosammonium ion, which has a diameter of approximately 10 Å, was essentially impermeable.

$(LSLLLSL)_3$ forms proton-selective channels. $(LSLLLSL)_3$ formed channels that were less conductive, of shorter open lifetime, and more selective than those formed by $(LSSLLSL)_3$. In 0.5*M* HCl, the channels formed by $(LSLLLSL)_3$ had a single major conductance state of 120 pS (Fig. 3D) as compared with a value of 900 pS for the channels formed by $(LSSLLSL)_3$ at the same voltage and HCl concentration. The average open lifetime (Fig. 3E) was about 1 ms. Closed times (Fig. 3F) were, as with the $(LSSLLSL)_3$ peptide, exponentially distributed and decreased with increasing voltage. Most strikingly, within the experimental detection limits

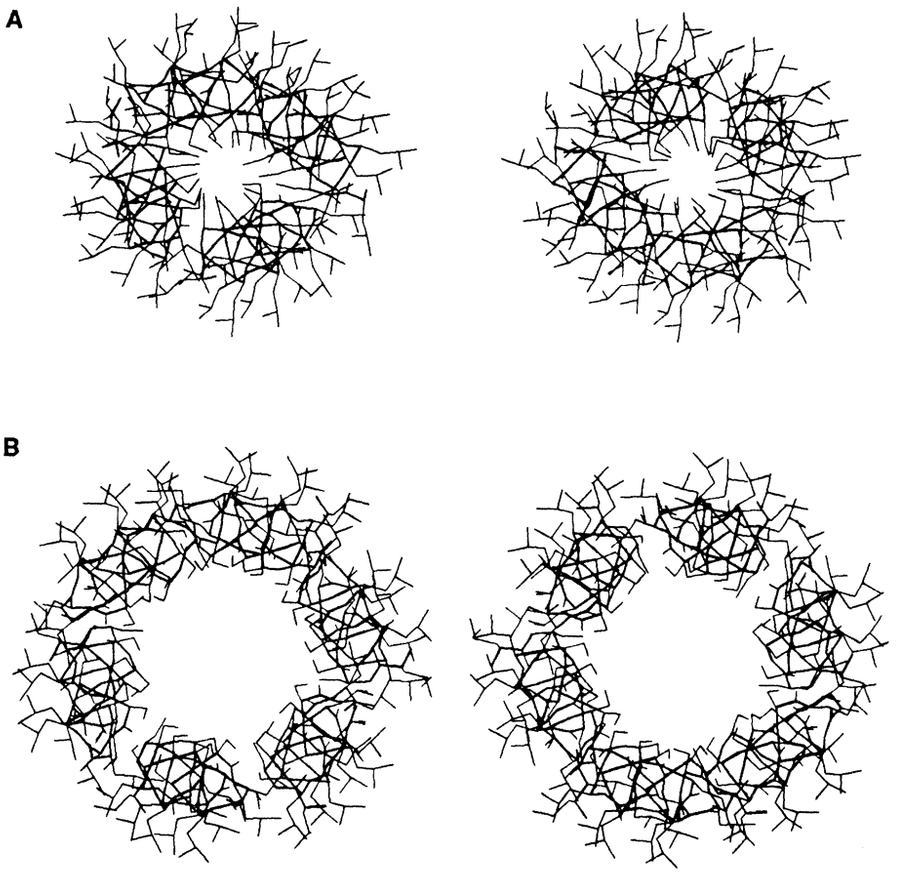

Fig. 4. Stereo-pair drawings of peptide ion channel models: (**A**) tetrameric model of $(LSLLLSL)_3$ and (**B**) hexameric model of $(LSSLLSL)_3$. The models were built by applying the transformations of the C_n point group (n is the aggregation number) to a single ideal α-helix with the computer graphics program MOLEDITOR (*38*), and the resulting bundle was given a left-handed twist to improve side chain packing (*29, 31*). Side chains were rotated to relieve steric interference, and the aggregated structure was energy minimized with a Cray 1-A computer and the program AMBER with a 9.5 Å cutoff for nonbonded interactions (*28*). After visual inspection, additional side chain rotations and energy minimizations were performed until no further improvements could be made with the criteria of low potential energy and closeness of fit between van der Waals surfaces of adjacent helices (*38*).

(approximately 5 pS), the channels formed by $(LSLLLSL)_3$ appeared to be impermeable to all of the other cations tested. For example, channels could not be observed with 10*M* LiCl, 5.0*M* NaCl, or 2.5*M* KCl. The bulk solution conductance of 10*M* LiCl is about twice that of 0.5*M* HCl, so if the channels were not selective, 10*M* LiCl would have given channel conductances of greater than 200 pS. Since we observed no conductance greater than the 5 pS detection limit when 0.5*M* HCl was replaced with 10*M* LiCl, we conclude that protons passed through the $(LSLLLSL)_3$ channels at least 40-fold more rapidly than lithium cations.

A molecular model for the channels. Computer graphics and energy minimization were used to create a number of molecular models for $(LSSLLSL)_3$ and $(LSLLLSL)_3$ in which the channel was formed by α-helices arranged in bundles with the polar side chains oriented toward the bundle center. The helices were oriented parallel to one another to create structures with the qualitative asymmetry suggested by the lack of symmetry in the formation of channels with respect to voltage reversal across the bilayer. Modeling efforts were generally aimed at achieving minimum energy conformations with close packing of side chains between neighboring helices. A variety of models of trimeric, tetrameric, pentameric, and hexameric helical bundles were constructed and then energy minimized (*28*); the resulting structures with the best side-chain packing and the lowest energies all had rotational symmetry. The side chains of neighboring helices packed together in a "knobs-into-holes" fashion (Fig. 4), as has been previously observed for a variety of helix-helix packings involving identical, parallel α-helices (*29–31*). A single, highly efficient packing (Fig. 5) was found for each aggregation number, and this packing was the same for both heptad sequences. Channel diameters for each structure were defined by calculating the maximum distance between van der Waals surfaces of serine side chains at the narrowest part of the channel. The trimeric channel is completely closed, and the tetrameric channel, with a diameter of less than 1 Å, is almost closed. Pentameric and hexameric channels have much larger diameters of 5 and 8 Å, respectively (Fig. 6). In the pentameric and hexameric models of $(LSSLLSL)_3$, the serine side chains can donate and accept hydrogen bonds (*32*) to water molecules in the channel, and the channels are wide enough to have waterlike interiors. In contrast, the trimeric and tetrameric models of $(LSLLLSL)_3$ have room for only isolated water molecules among the serine side chains in the interior of the channel.

The characteristics of the models, combined with the measured conduction rates of various sized cations, lead us to the working hypothesis that the channel formed by $(LSLLLSL)_3$ is a trimeric or tetrameric aggregate, whereas that formed by $(LSSLLSL)_3$ is a hexameric or possibly larger aggregate. An explanation for the postulated tendency of $(LSSLLSL)_3$ to form higher aggregates than $(LSLLLSL)_3$ can be inferred from an examination of the trimeric and tetrameric (Fig. 4) models for $(LSLLLSL)_3$. In these structures the leucine at position 3 of each heptad repeat (Fig. 1, B and C) packs between leucyl side chains of a neighboring helix in a knobs-into-holes fashion (*29*). Replacement of this large, apolar side chain with the smaller, polar seryl side chain could be expected to destabilize the interhelical packing. Thus $(LSSLLSL)_3$ might be expected to form annular structures with larger radii to mitigate this otherwise unfavorable interaction, as well as to allow more complete hydration of the seryl hydroxyls.

Implications to the structures of ion channel proteins. The ion channel conductance, lifetime, and cation selectivity of $(LSSLLSL)_3$ are strikingly similar to those of the acetylcholine receptor (Table 1). The drastic difference in conduction properties between $(LSSLLSL)_3$ and $(LSLLLSL)_3$ show how a seemingly minor perturbation in amino acid sequence can give rise to large functional

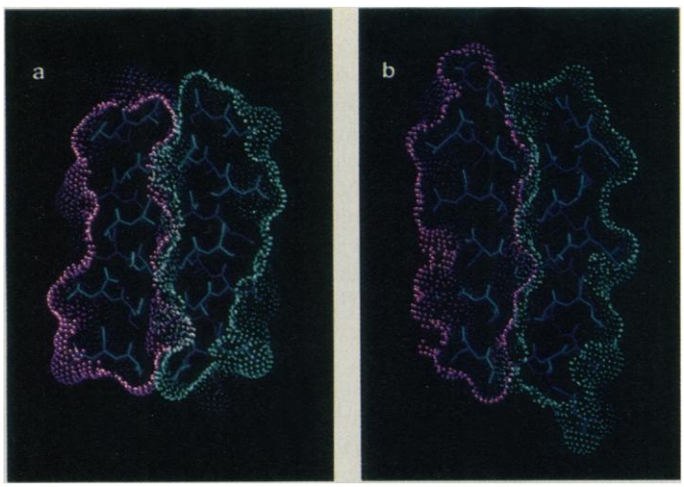

Fig. 5. Representative side views of the interhelical packing: (**A**) tetrameric model of $(LSLLLSL)_3$ and (**B**) hexameric model of $(LSSLLSL)_3$. Purple and blue dots show the molecular surfaces calculated with the Connolly algorithm (*39*) for two adjacent helices; note the good geometric fit. Because of the rotational symmetry of the models, all of the interhelical packings in a given model are identical.

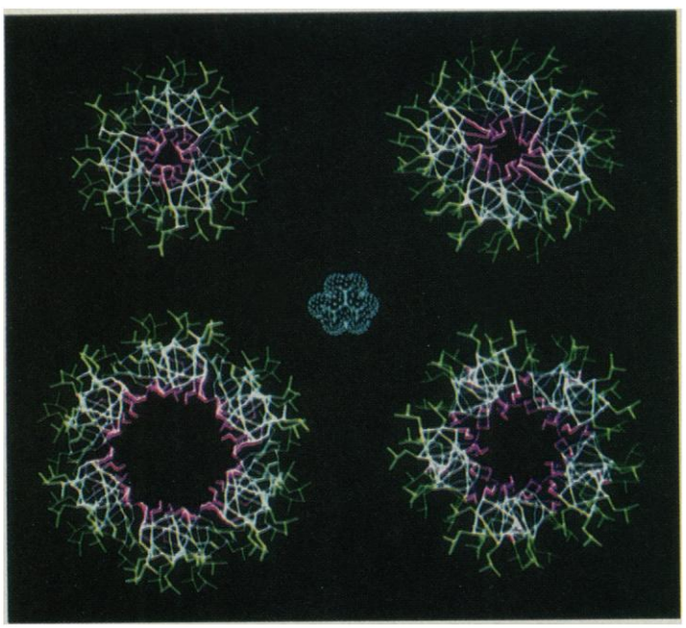

Fig. 6. Axial views of the trimeric and tetrameric models of $(LSLLLSL)_3$ and of the pentameric and hexameric models of $(LSSLLSL)_3$. Backbone atoms (C_α, C, and N) are shown in white, leucine side chains in green, and serine side chains in purple. For size comparison, a van der Waals surface representation of the guanidinium ion is shown as a dotted surface at the center of the diagram.

changes, and illustrates how functional diversity can be generated within a simple structural paradigm. Both peptides form ion channels similar to those of complex natural proteins, which provides support for models of natural ion channels in which the ion conduction pathway is composed of transmembrane helical segments with aggregated, neutral, polar faces (*9, 33*). The large difference in conductance and ion selectivity between our two model channel peptides suggests that interhelical side chain packing and the degree of polar side chain exclusion from the hydrophobic membrane environment both interact to influence the size and structure of the channel interior, and hence its function. It would be helpful in the analysis of natural channels to determine whether these principles can be used to design new channel peptides with different ion selectivities.

REFERENCES AND NOTES

1. B. Hille, *Ionic Channels of Excitable Membranes* (Sinauer, Sunderland, MA, 1984).
2. M. Noda *et al.*, *Nature* **302**, 528 (1983).
3. P. R. Schofield *et al.*, *ibid.* **328**, 221 (1987).
4. G. Grenningloh *et al.*, *ibid.* p. 215.
5. M. Noda *et al.*, *ibid.* **312**, 121 (1984).
6. D. M. Papazian, T. L. Schwarz, B. L. Tempel, Y. N. Jan, L. Y. Jan, *Science* **237**, 749 (1987).
7. T. Tanabe *et al.*, *Nature* **328**, 313 (1987).
8. H. R. Guy, *Biophys. J.* **45**, 249 (1984); J. Finer-Moore and R. Stroud, *Proc. Natl. Acad. Sci. U.S.A.* **81**, 155 (1984); R. E. Greenblatt, Y. Blatt, M. Montal, *FEBS Lett.* **193**, 125 (1985).
9. H. R. Guy and F. Hucho, *Trends Neurosci.* **10**, 318 (1987).
10. P. Mueller and D. O. Rudin, *Nature* **217**, 713 (1968); R. O. Fox and F. M. Richards, *ibid.* **300**, 325 (1982).
11. M. T. Tosteson and D. C. Tosteson, *Biophys. J.* **36**, 109 (1981); W. Hanke *et al.*, *Biochim. Biophys. Acta* **727**, 108 (1983).
12. B. V. Prasad and P. Balaram, *CRC Crit. Rev. Biochem.* **16**, 307 (1983).
13. M. T. Tosteson *et al.*, *Biochemistry* **26**, 6627 (1987).
14. G. Spach, Y. Trudelle, F. Heitz, *Biopolymers* **22**, 403 (1983); G. Spach, Y. Merle, G. Molle, *J. Chim. Phys.* **82**, 719 (1985).
15. D. Eisenberg, E. Schwartz, M. Komorany, R. Wall, *J. Mol. Biol.* **179**, 125 (1984).
16. D. M. Engleman, T. A. Steitz, A. Goldman, *Annu. Rev. Biophys. Chem.* **15**, 321 (1986).
17. P. Y. Chou and G. D. Fasman, *Annu. Rev. Biochem.* **47**, 251 (1978).
18. W. F. DeGrado and E. T. Kaiser, *J. Org. Chem.* **47**, 3258 (1982); W. F. DeGrado and J. D. Lear, *J. Am. Chem. Soc.* **107**, 7684 (1985).
19. N. Greenfield and G. D. Fasman, *Biochemistry* **8**, 4108 (1969).
20. Diphytanoyl phosphatidylcholine bilayers were made by monolayer apposition [M. Montal and P. Mueller, *Proc. Natl. Acad. Sci. U.S.A.* **69**, 3561 (1972)]. The peptides were incorporated by adding 1 to 5 μl of a solution of the peptides (0.1 mg/ml) in methanol or dimethyl sulfoxide to one side of the bilayer (aqueous volume 2 ml). To promote the incorporation of the peptide into the bilayer [R. U. Muller and O. S. Anderson, *J. Gen. Physiol.* **80**, 427 (1982)], the bilayer was broken and reformed before the data were collected. Once the peptide was incorporated, the aqueous solution could be replaced with pure electrolyte solutions and the channels were still present.
21. R. Blumenthal and R. D. Klausner, in *Membrane Reconstitution*, G. Poste and G. L. Nicolson, Eds. (Elsevier, New York, 1982), p. 61; C. Kempf *et al.*, *J. Biol. Chem.* **257**, 2469 (1987).
22. Data were analyzed by a program written for an MS-DOS 80286 computer. A listing of the program and more detailed information are available from the authors.
23. Single channel records varied considerably in quality. Records with erratic occurrences of current fluctuations superimposed on channel activity were discarded. In some cases, a considerable fraction of channels with lower conductances than the main peaks was observed shortly after addition of the peptide. Such channels tended to disappear within minutes to hours, whereas the larger channels remained or increased in frequency.
24. D. Colquhoun and A. G. Hawkes, in *Single Channel Recording*, B. Sakmann and E. Neher, Eds. (Plenum, New York, 1983), p. 135.
25. In a given experiment, the frequency of channel openings at fixed voltage could be increased by adding more peptide to the electrolyte solution. The frequency could also be reduced by perfusion with fresh electrolyte, but this required many solution replacements and long times, indicative of very strong association of the peptides with lipid or the chamber surfaces or both.
26. B. Honig, W. L. Hubbell, R. F. Fleming, *Annu. Rev. Biophys. Biophys. Chem.* **15**, 163 (1986).
27. B. Hille, in (*1*), p. 247.
28. P. K. Weiner *et al.*, *J. Am. Chem. Soc.* **106**, 765 (1984).
29. F. H. C. Crick, *Acta Cryst.* **6**, 689 (1953); C. Cohen and D. A. Parry, *Trends Biochem. Sci.* **11**, 245 (1986).
30. I. Wilson, J. J. Skehel, D. Wiley, *Nature* **289**, 366 (1981).
31. D. W. Banner, M. Kokkinidis, D. Tsernoglost, *J. Mol. Biol.* **196**, 657 (1987).
32. E. N. Baker and R. E. Hubbard, *Prog. Biophys. Mol. Biol.* **44**, 97 (1984).
33. S. Furois-Corbin and A. Pullman, *Biochim. Biophys. Acta* **902**, 31–45 (1987); N. Burres and A. K. Dunker, *J. Theor. Biol.* **87**, 723–736 (1980).
34. P. H. Barry and P. W. Gage, *Curr. Topics Membranes Transport* **21**, 1 (1984).
35. S. H. Heinemann, W. Stuhmer, F. Conti, *Proc. Natl. Acad. Sci. U.S.A.* **84**, 3229 (1987).
36. R. W. Aldrich, D. P. Corey, C. F. Stevens, *Nature* **306**, 43 (1983).
37. T. M. Dwyer, D. J. Adams, B. Hille, *J. Gen. Physiol.* **75**, 469 (1980).
38. Model building and stereo drawings were created with the computer program MOLEDITOR(copywrite), written by R. Hilmer of Du Pont.
39. M. L. Connolly, *Science* **221**, 709 (1983).

40. We gratefully acknowledge the assistance of I. Turner in the synthesis and purification of peptides, and of J. Kallal in writing the channel analysis programs. We thank M. Tosteson for helpful advice in making planar bilayers, R. Salemme for providing molecular modeling facilities and insightful guidance, M. Montal for constructive comments, and C. Farber for preparing this manuscript.

8 February 1988; accepted 18 April 1988